Supporting Information

Apparatus

Eye movements were recorded at 1000 Hz using an EyeLink 1000 Plus eye tracker (SR Research Ltd., Mississauga, Ontario, Canada) in order to identify fixations. Fixations were scored when >100 ms elapsed without a blink or a saccade. (When a fixation <100 ms in duration occurred within 0.5° of another fixation, the two were counted as a single fixation if the total duration of the two exceeded 100 ms). A blink was scored when the image of the pupil was lost. A saccade was defined as an eye movement of at least 0.5° that occurred with a velocity exceeding 30°/s or an acceleration exceeding 8000°/s^2. Head motion and position were maintained with a forehead and chin rest. The eye tracker was calibrated at the beginning of each test block by mapping the correspondence between 13 target locations and the direction of gaze when participants viewed each location. In addition, adjustments for head motion were carried out between trials when gaze direction drifted by > 0.2°. Participants made their responses on an external keyboard. A separate computer controlled scene presentation and recorded behavioral responses using EyeLink Experiment Builder software (version 1.10.1630). Stimuli were presented on an 18-in monitor (1920 x 1200 resolution) positioned 74 cm from the participant.

Etiology and quantitative measurements of brain lesions of MTL patients

Patients G.W. and D.A. became amnesic in 2001 and 2011, respectively, following a drug overdose and associated respiratory failure. K.E. became amnesic in 2004 after an episode of ischemia associated with kidney failure and toxic shock syndrome. L.J. (the only female) became amnesic during a 6-mo period in 1988 with no known precipitating event. Her memory impairment has been stable since that time. G.P. has severe memory impairment resulting from viral encephalitis in 1987.

Estimates of MTL damage were based on quantitative analysis of magnetic resonance (MR) images from 19 age-matched, healthy males for K.E., G.W., and G.P., 11 age-matched, healthy females for patient L.J. (1), and 8 younger healthy males for D.A.. Patients D.A., K.E., L.J., and G.W. have an average bilateral reduction in hippocampal volume of 35, 49, 46, and 48%, respectively (all values at least 2.9 SDs from the control mean). On the basis of two patients (L.M. and W.H.) with similar bilateral volume loss in the hippocampus for whom detailed postmortem neurohistological information was obtained (2) the degree of volume loss in the four hippocampal patients may reflect nearly complete loss of hippocampal neurons. The volume of the parahippocampal gyrus (temporopolar, perirhinal, entorhinal, and parahippocampal cortices) is reduced by -5, 11, -17, and 10%, respectively (all values within 2 SDs of the control mean). The negative values indicate volumes that were larger for a patient than for controls. These values are based on published guidelines for identifying the boundaries of the parahippocampal gyrus (3, 4).

G.P. has an average bilateral reduction in hippocampal volume of 96%. The volume of the parahippocampal gyrus is reduced by 94%. G.P. also has a reduction of 24% (> 3 SDs below control mean) in the left lateral temporal lobe and a reduction of 6% (< 1 SD below control mean) in the right temporal lobe. The volumes of the lateral temporal lobes were calculated for G.P. and 14 age-matched controls using FreeSurfer software (version 5.1; 5, 6-8). The temporal lobe measures included gray matter and associated white

matter from fusiform, inferior temporal, middle temporal, and superior temporal gyri. The volumes were adjusted with respect to intracranial volume as calculated by FreeSurfer (estimated total intracranial volume; 9). Manual intervention was carried out to correct errors associated with boundaries between the brain and pia/skull and boundaries between gray matter and white matter. Eight coronal magnetic resonance images from each patient, together with detailed descriptions of the MTL lesions, can be found in Figure S1.

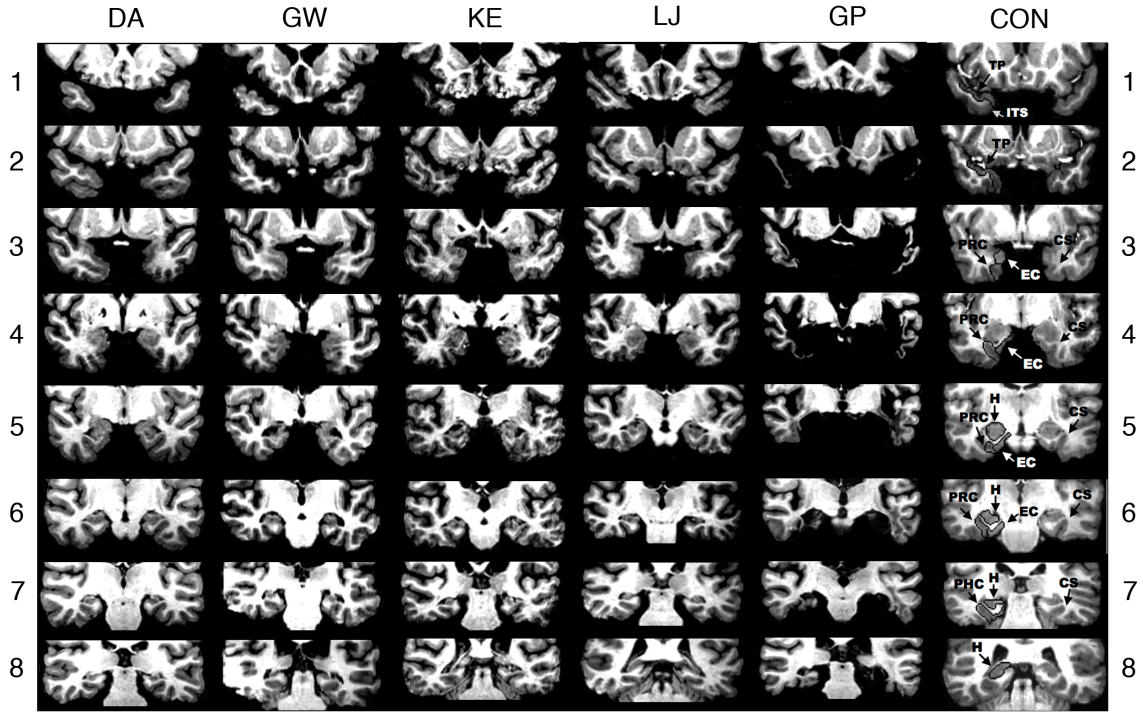

Figure S1. Series of eight T1-weighted coronal images of six patients are illustrated with limited hippocampal lesions (DA, GW, KE, and LJ), one patient with extensive medial temporal lobe damage (GP), and one control (CON). The sections proceed posteriorly in 7mm intervals from the temporopolar (TP) cortex in the top section. The left side of the brain is on the right side of each image.

As described by ref (3), TP cortex extends medially from the inferotemporal sulcus (ITS) to the fundus of the TP sulcus. TP cortex extends rostrally from the tip of the temporal pole caudally to the limen insula (LI), which approximates the border between the TP cortex and perirhinal cortex (PRC). Caudal to TP cortex, the collateral sulcus (CS) is the most important structure for the identification of medial temporal lobe cortices. At its most rostral extent, the CS is surrounded entirely by PRC. Caudally, entorhinal cortex (EC) extends from the midpoint of the medial bank of the CS to the subiculum, while PRC extends laterally from the midpoint of the medial bank of the CS to the inferotemporal cortex. Two millimeters caudal to the disappearance of the gyrus intralimbicus of the hippocampus (H), the CS is surrounded by parahippocampal cortex (PHC). The caudal border of the posterior PHC is defined as lying 1.5mm posterior to the

crus of the fornix at the point where the fimbria turns upwards to continue as the posterior pillars of the fornix and posterior to the pulvinar nucleus of the thalamus (ref 4).

The top section (1) shows the TP cortex and the ITS in the control brain. None of the patients with limited hippocampal lesions have damage evident at this level. For GP, the TP cortex and lateral temporal cortex are missing bilaterally. The ITS is visible bilaterally at this level for patients GW and KE. For LJ, only the right ITS is visible. For DA, the ITS is not visible on either side at this level. The second section (2) shows TP cortex and the ITS in the control brain. The ITS and TP cortex is evident in all patients with limited hippocampal lesions at this level. None of the patients with limited hippocampal lesions has damage evident at this level. For GP, note that the portion of the temporal lobe missing corresponds to TP cortex and also involves the lateral temporal lobe, especially on the left. The CS is visible, indicating the beginning of PRC, in patients KE (right side only). The third section (3) shows the CS and surrounding PRC and EC in the control brain. None of the patients with limited hippocampal lesions has damage evident at this level with the exception of KE, who has damage in the basal ganglia secondary to toxic shock syndrome (and to a lesser extent in section 4). For patient DA, the CS is not evident at this level and PRC is evident bilaterally. For patients GW, KE, and LJ, the PRC is evident on the left side, bounded by the LI and CS. On the right side, both EC and PRC are evident. For GP, no CS or surrounding tissue is evident, and damage to left lateral temporal lobe is evident. The fourth section (4) shows the anterior hippocampus and the adjacent PRC and EC in the control brain. At this level hippocampal damage is evident in patient DA. The hippocampus is not yet visible at this level in any of the other patients with limited hippocampal lesions. For DA, bilateral damage to the globus pallidus is evident at this level, presumably secondary to heroin overdose. No damage to the PRC or EC is evident for any of the patients at this level, except for GP who has no medial temporal lobe tissue at this level and who has damage to the left lateral temporal lobe. The fifth section (5) shows the hippocampus and the adjacent PRC and EC in the control brain. The CS and the surrounding PRC and EC appear normal in all patients at this level with the exception of GP, who has no medial temporal lobe tissue at this level and who exhibits some damage to left lateral temporal lobe. Damage is evident in the hippocampal region of all patients. The sixth section (6) shows the hippocampus and the adjacent PRC and EC in the control brain. Damage is evident in the hippocampal region for all patients at this level. The surrounding PRC and EC appear normal in all patients except GP, who has little normal medial temporal lobe tissue in either hemisphere. Both the PRC and EC are visible in all hippocampal patients bilaterally. The seventh section (7) shows the hippocampus and the CS, surrounded by PHC in the control brain. Damage to the hippocampus is evident in all patients at this level. In all patients with damage limited to the hippocampus, the PHC is evident, but in patient DA the PRC is still visible on the right side. Patient GP has little normal medial temporal lobe tissue in either hemisphere. The eighth section (8) shows the hippocampus in the control brain. Bilateral hippocampal damage is evident in patients DA, GW, KE, and GP at this level. Patient LJ shows hippocampal damage only on the left side. PHC is no longer evident at this level in patients DA, KE, or LJ and PHC appears normal in patient GW. Patient GP has some spared PHC on the right at this level. The warping artifact in the right lateral temporal lobe of GW on this section did not interfere with the assessment of his damage. Posterior to this level, GP exhibits hippocampal damage and damage to the PHC. No damage is evident posterior to this level for any of the other patients.

References

1. Gold JJ, Squire LR (2005) Quantifying medial temporal lobe damage in memory-impaired patients. *Hippocampus* 15(1):79-85.
2. Rempel-Clower NL, Zola SM, Squire LR, Amaral DG (1996) Three cases of enduring memory impairment after bilateral damage limited to the hippocampal formation. *J. Neurosci.* 16(16):5233-5255.
3. Insausti R*, et al.* (1998) MR volumetric analysis of the human entorhinal, perirhinal, and temporopolar cortices. *Am. J. Neuroradiol.* 19(4):659-671.
4. Franko E, Insausti AM, Artacho-Perula E, Insausti R, Chavoix C (2014) Identification of the human medial temporal lobe regions on magnetic resonance images. *Hum. Brain Mapp.* 35(1):248-256.
5. Fischl B*, et al.* (2002) Whole Brain Segmentation: Automated Labeling of Neuroanatomical Structures in the Human Brain. *Neuron* 33:341-355.
6. Fischl B, Sereno MI, Dale AM (1999) Cortical surface-based analysis. II: Inflation, flattening, and a surface-based coordinate system. *NeuroImage* 9(2):195-207.
7. Fischl B*, et al.* (2004) Automatically Parcelling the Human Cerebral Cortex. *Cereb. Cortex* 14(1):11-22.
8. Dale AM, Fischl B, Sereno MI (1999) Cortical surface-based analysis. I. Segmentation and surface reconstruction. *NeuroImage* 9(2):179-194.
9. Buckner RL*, et al.* (2004) A unified approach for morphometric and functional data analysis in young, old, and demented adults using automated atlas-based head size normalization: reliability and validation against manual measurement of total intracranial volume. *NeuroImage* 23:724-738.